

Electronic Supplementary Information (ESI)

Supramolecular assemblies of Zn(II) complexes with D- π -A ligand for sensing specific organic molecules

Zi-Qing Huang,^a Jia-Qi Chen,^a Shu-Man Zhao,^a Zhao-Feng Qiu,^b Yue Zhao^a and Wei-Yin Sun^{*a}

^a Coordination Chemistry Institute, State Key Laboratory of Coordination Chemistry, School of Chemistry and Chemical Engineering, Nanjing National Laboratory of Microstructures, Collaborative Innovation Center of Advanced Microstructures, Nanjing University, Nanjing 210023, China. E-mail: sunwy@nju.edu.cn; Tel: +86 25 89683485

^b College of Chemistry and Environmental Engineering, Yangtze University, Jingzhou 434023, China.

* Corresponding author.

Email address: sunwy@nju.edu.cn (W. Y. Sun)

EXPERIMENTAL

X-ray crystallography. Single-crystal X-ray diffraction data were collected on a Bruker D8 Venture diffractometer with graphite-monochromated Mo K α radiation ($\lambda = 0.71073$ Å). The integration of diffraction data and intensity corrections for the Lorentz and polarization effects were performed by using SAINT program.¹ Semi-empirical absorption corrections were applied using SADABS program.² The structures were solved by direct methods with SHELXT-2014, expanded by subsequent Fourier-difference synthesis, and all the non-hydrogen atoms were refined anisotropically on F^2 using the full-matrix least-squares technique with the SHELXL-2018 crystallographic software package.^{3,4} The free solvent molecules in the unit cell

have been taken into account by SQUEEZE option of the PLATON program.⁵ The final chemical formulas were determined by volume/count electrons, elemental and TGA. The reported refinements are of the guest-free structures obtained by the SQUEEZE routine and the results were attached to the CIF files. The details of crystal parameters, data collection and refinements for **1**, **2** and **3** are listed in **Table 1**, and the selected bond lengths and angles are given in **Table S1**.

Theoretical calculations. First principle DFT calculations were carried out by using the Dmol3 module in Material Studio software package.⁶ The initial configuration was fully optimized based on crystal structures of **1**, **2**, **3** and single molecular TNP by the Perdew-Burke-Ernzerhof (GGA-PBE) exchange correlation functional sets with spin-polarization, which is required to describe weak interactions.⁷⁻⁹ The self-consistent field converged criterion was 1.0×10^{-5} hartree atom⁻¹, and the converging criterion of structure optimization was 1.0×10^{-3} hartree bohr⁻¹. The Brillouin zone was sampled by $1 \times 1 \times 1$ k-points, and test calculations reveal that the increase of k-points does not affect the results.

Table S1 Selected bond lengths (Å) and angles (°) for **1**, **2** and **3**.

1			
Zn(1)-N(4)	2.220(3)	Zn(1)-N(5)	2.071(2)
Zn(1)-N(6)	2.188(3)	Zn(1)-N(7)	2.212(2)
Zn(1)-N(8)	2.082(2)	Zn(1)-N(9)	2.168(2)
N(5)-Zn(1)-N(4)	75.08(9)	N(5)-Zn(1)-N(6)	76.03(9)
N(5)-Zn(1)-N(7)	97.39(9)	N(5)-Zn(1)-N(8)	172.54(9)
N(5)-Zn(1)-N(9)	111.94(9)	N(6)-Zn(1)-N(7)	94.79(9)
N(6)-Zn(1)-N(4)	150.96(10)	N(7)-Zn(1)-N(4)	91.71(9)
N(8)-Zn(1)-N(6)	104.53(9)	N(8)-Zn(1)-N(7)	75.16(9)
N(8)-Zn(1)-N(4)	104.49(10)	N(8)-Zn(1)-N(9)	75.49(9)
N(9)-Zn(1)-N(6)	95.15(9)	N(9)-Zn(1)-N(7)	150.51(9)
N(9)-Zn(1)-N(4)	92.91(9)		
2			
Zn(1)-O(4)	1.962 (2)	Zn(1)-O(1)	1.969(2)
Zn(1)-N(3)	2.224(3)	Zn(1)-N(4)	2.081(2)
Zn(1)-N(5)	2.234(3)		
O(4)-Zn(1)-O(1)	120.78(9)	O(4)-Zn(1)-N(4)	111.12(9)
O(4)-Zn(1)-N(5)	96.83(9)	O(4)-Zn(1)-N(3)	101.24(10)
O(1)-Zn(1)-N(4)	128.09(9)	O(1)-Zn(1)-N(5)	99.32(9)
O(1)-Zn(1)-N(3)	93.84(10)	N(4)-Zn(1)-N(5)	74.15(10)
N(4)-Zn(1)-N(3)	74.76(10)	N(3)-Zn(1)-N(5)	147.99(10)
3			
Zn(1)-O(4)	1.9464(15)	Zn(1)-O(2)	1.9585(15)
Zn(1)-N(3)	2.1022(17)	Zn(1)-N(2)	2.2086(18)
Zn(1)-N(4)	2.2325(18)		
O(4)-Zn(1)-O(2)	120.05(6)	O(4)-Zn(1)-N(3)	108.51(7)
O(4)-Zn(1)-N(2)	103.98(7)	O(4)-Zn(1)-N(4)	92.93(6)
O(2)-Zn(1)-N(3)	131.43(6)	O(2)-Zn(1)-N(2)	93.48(6)
O(2)-Zn(1)-N(4)	101.92(7)	N(3)-Zn(1)-N(2)	74.31(6)
N(3)-Zn(1)-N(4)	73.98(6)	N(2)-Zn(1)-N(4)	147.44(7)

Table S2 The member atoms of conjugate rings for **1**, **2** and **3**. (CgI = plane number I).

1						
CgI	Ring member atoms					
Cg1	Zn1	N4	C19	C18	N5	
Cg2	Zn1	N5	C14	C13	N6	
Cg3	Zn1	N7	C28	C29	N8	
Cg4	Zn1	N8	C33	C34	N9	
Cg5	N1	C47	N3	N2	C48	
Cg6	N10	N11	C2	N12	C1	
Cg7	N4	C19	C20	C21	C22	C23
Cg8	N5	C14	C15	C16	C17	C18
Cg9	N6	C9	C10	C11	C12	C13
Cg10	N7	C24	C25	C26	C27	C28
Cg11	N8	C29	C30	C31	C32	C33
Cg12	N9	C34	C35	C36	C37	C38
Cg13	C3	C4	C5	C6	C7	C8
Cg14	C39	C40	C41	C42	C43	C44

2						
CgI	Ring member atoms					
Cg3	Zn1A	O1	C6	O2		
Cg4	Zn1	N3	C17	C18	N4	
Cg5	Zn1	N4	C22	C23	N5	
Cg6	N6	C34	N8	N7	C35	
Cg7	N1	C1	C2	C3	C4	C5
Cg8	N2	C10	C9	C8	C12	C11
Cg9	N3	C13	C14	C15	C16	C17
Cg10	N4	C18	C19	C20	C21	C22
Cg11	N5	C23	C24	C25	C26	C27
Cg12	C28	C29	C30	C31	C32	C33

3						
CgI	Ring member atoms					
Cg1	Zn1	N2	C19	C18	N3	
Cg2	Zn1	N3	C11	C12	N4	
Cg3	N5	N6	C1	N7	C2	
Cg4	N1	C28	C27	C26	C30	C29
Cg5	N2	C19	C20	C21	C22	C23
Cg6	N3	C11	C10	C9	C17	C18
Cg7	N4	C12	C13	C14	C15	C16
Cg8	C3	C4	C5	C6	C7	C8

Table S3 The Cg-Cg distances (Å) between ring centroids for **1**, **2** and **3**.

1					
	CgI->CgJ	Distance		CgI->CgJ	Distance
1	Cg1->Cg7 #1	4.5638 (17)	22	Cg1->Cg10 #2	4.2112 (18)
2	Cg1->Cg12 #2	4.4870 (18)	23	Cg2->Cg10 #2	4.2163 (19)
3	Cg2->Cg12 #2	4.4927 (18)	24	Cg3->Cg5 #5	4.4197 (19)
4	Cg3->Cg7 #2	4.2965 (17)	25	Cg3->Cg9 #2	4.3678 (18)
5	Cg3->Cg12 #3	4.8883 (19)	26	Cg4->Cg6 #7	4.8967 (19)
6	Cg4->Cg7 #1	4.4145 (18)	27	Cg4->Cg9 #2	4.3979 (18)
7	Cg4->Cg10 #4	4.8897 (19)	28	Cg5->Cg3 #5	4.4196 (19)
8	Cg5->Cg10 #5	3.852 (2)	29	Cg5->Cg11 #6	4.9993 (19)
9	Cg5->Cg14 #6	3.723 (2)	30	Cg6->Cg4 #7	4.8967 (19)
10	Cg6->Cg12 #7	3.676 (2)	31	Cg6->Cg13 #9	3.803 (2)
11	Cg7->Cg1 #1	4.5637 (17)	32	Cg7->Cg7 #1	4.0946 (19)
12	Cg7->Cg8 #1	4.9034 (18)	33	Cg7->Cg12 #3	4.962 (2)
13	Cg8->Cg7 #1	4.9035 (18)	34	Cg9->Cg13 #8	4.927 (2)
14	Cg9->Cg13 #5	4.677 (2)	35	Cg10->Cg4 #3	4.8896 (19)
15	Cg10->Cg5 #5	3.852 (2)	36	Cg10->Cg12 #3	3.563 (2)
16	Cg10->Cg13 #5	4.374 (2)	37	Cg11->Cg5 #9	4.9995 (19)
17	Cg12->Cg3 #4	4.8884 (19)	38	Cg12->Cg6 #7	3.676 (2)
18	Cg12->Cg10 #4	3.563 (2)	39	Cg13->Cg6 #6	3.803 (2)
19	Cg13->Cg9 #8	4.927 (2)	40	Cg13->Cg10 #5	4.374 (2)
20	Cg13->Cg14 #6	4.793 (2)	41	Cg14->Cg5 #9	3.723 (2)
21	Cg14->Cg13 #9	4.793 (2)			

2					
	CgI->CgJ	Distance		CgI->CgJ	Distance
1	Cg3->Cg10 #1	4.957 (3)	13	Cg7->Cg12 #1	4.507 (2)
2	Cg3->Cg11 #1	4.856 (3)	14	Cg8->Cg9 #2	4.764 (2)
3	Cg6->Cg7 #3	4.211 (2)	15	Cg9->Cg8 #4	4.944 (2)
4	Cg7->Cg6 #5	4.211 (2)	16	Cg10->Cg3 #1	4.957 (3)
5	Cg8->Cg9 #6	4.944 (2)	17	Cg11->Cg3 #1	4.856 (3)
6	Cg9->Cg7 #7	4.905 (2)	18	Cg11->Cg6 #6	4.821 (2)
7	Cg9->Cg8 #2	4.764 (2)	19	Cg11->Cg10 #1	3.7287 (19)

8	Cg10->Cg11 #1	3.7285 (19)	20	Cg11->Cg11 #1	4.491 (2)
9	Cg11->Cg4 #1	3.8523 (18)	21	Cg11->Cg10 #6	3.6942 (19)
10	Cg3->Cg11 #8	4.270 (3)	22	Cg12->Cg7 #1	4.507 (2)
11	Cg4->Cg11 #1	3.8523 (18)	23	Cg12->Cg11 #4	3.6943 (19)
12	Cg6->Cg11 #4	4.821 (2)			

3

	CgI->CgJ	Distance		CgI->CgJ	Distance
1	Cg1->Cg7 #1	3.8704 (12)	12	Cg5->Cg4 #8	4.9432 (12)
2	Cg2->Cg7 #1	3.4880 (12)	13	Cg6->Cg7 #1	3.8434 (12)
3	Cg3->Cg3 #2	3.8092 (18)	14	Cg7->Cg2 #1	3.4880 (12)
4	Cg3->Cg7 #3	4.9161 (14)	15	Cg7->Cg3 #5	4.9161 (14)
5	Cg4->Cg8 #1	4.5293 (13)	16	Cg7->Cg6 #1	3.8434 (12)
6	Cg5->Cg8 #4	3.6999 (13)	17	Cg7->Cg7 #1	4.4205 (12)
7	Cg7->Cg1 #1	3.8705 (12)	18	Cg7->Cg8 #5	3.6631 (12)
8	Cg2->Cg2 #1	3.9608 (12)	19	Cg8->Cg2 #3	4.8088 (11)
9	Cg2->Cg8 #5	4.8087 (11)	20	Cg8->Cg5 #4	3.6999 (13)
10	Cg3->Cg4 #6	4.2854 (16)	21	Cg8->Cg7 #3	3.6632 (12)
11	Cg4->Cg3 #7	4.2854 (16)			

Symmetry codes: #1 1-x,-y,1-z; #2 x,y,z; #3 1+x,y,z; #4 -1+x,y,z; #5 1-x,1-y,1-z; #6 x,y,1+z; #7 1-x,-y,-z; #8 -x,1-y,1-z; #9 x,y,-1+z for **1**; #1 -x,1-y,1-z; #2 -x,1-y,-z; #3 1+x,1+y,z; #4 1+x,y,z; #5 -1+x,-1+y,z; #6 -1+x,y,z; #7 -x,-y,1-z; #8 x,y,z for **2**; #1 2-x,1-y,1-z; #2 -x,2-y,-z; #3 -1+x,y,z; #4 1-x,2-y,1-z; #5 1+x,y,z; #6 -1+x,y,-1+z; #7 1+x,y,1+z; #8 2-x,1-y,2-z for **3**.

Table S4 Hydrogen bonding data of **1**, **2** and **3**.

1				
<i>D</i> -H... <i>A</i>	<i>d</i> (<i>D</i> -H) / Å	<i>d</i> (H... <i>A</i>) / Å	<i>d</i> (<i>D</i> ... <i>A</i>) / Å	<i>D</i> -H... <i>A</i> / °
C(2)-H(2)···O(6) #1	0.95	2.56	3.337(4)	139
C(8)-H(8)···O(4) #2	0.95	2.46	3.357(15)	157
C(12)-H(12)···O(5) #3	0.95	2.60	3.330(4)	134
C(12)-H(12)···O(7) #3	0.95	2.58	3.399(5)	144
C(15)-H(15)···O(7) #3	0.95	2.47	3.369(4)	159
C(17)-H(17)···N(13) #4	0.95	2.36	3.280(4)	163
C(24)-H(24)···O(7) #5	0.95	2.53	3.268(5)	134
C(27)-H(27)···O(2) #6	0.95	2.49	3.332(11)	147
C(27)-H(27)···O(3A) #6	0.95	2.41	3.353(15)	171
C(30)-H(30)···O(3A) #6	0.95	2.58	3.522(17)	174
C(35)-H(35)···O(2A) #3	0.95	2.51	3.423(11)	160
C(38)-H(38)···O(6) #7	0.95	2.57	3.178(4)	122
C(44)-H(44)···O(3) #3	0.95	2.42	3.163(15)	135
C(47)-H(47)···O(4) #2	0.95	2.39	3.325(16)	167
2				
<i>D</i> -H... <i>A</i>	<i>d</i> (<i>D</i> -H) / Å	<i>d</i> (H... <i>A</i>) / Å	<i>d</i> (<i>D</i> ... <i>A</i>) / Å	<i>D</i> -H... <i>A</i> / °
C(25)-H(25)···N(1) #3	0.93	2.53	3.432(5)	163
C(26)-H(26)···O(2) #4	0.93	2.43	3.352(4)	169
C(29)-H(29)···O(4) #5	0.93	2.50	3.271(4)	140
C(35)-H(35)···O(3) #6	0.93	2.46	3.271(6)	145
3				
<i>D</i> -H... <i>A</i>	<i>d</i> (<i>D</i> -H) / Å	<i>d</i> (H... <i>A</i>) / Å	<i>d</i> (<i>D</i> ... <i>A</i>) / Å	<i>D</i> -H... <i>A</i> / °
C(2)-H(2)···O(3) #1	0.95	2.39	3.234(4)	147
C(7)-H(7)···O(4) #2	0.95	2.38	3.188(2)	143
C(8)-H(8)···O(3) #1	0.95	2.58	3.401(3)	145
C(14)-H(14)···N(1) #3	0.95	2.56	3.478(3)	163
C(15)-H(15)···O(1) #4	0.95	2.41	3.340(3)	166

Symmetry codes: #1 1+x,y,-1+z; #2 -x,1-y,2-z; #3 -x,1-y,1-z; #4 x,y,1+z; #5 1+x,y,z; #6 1-x,1-y,1-z; #7 x,y,z for **1**; #1 -1-x,-y,1-z; #2 -1-x,1-y,-z; #3 x,1+y,z; #4 -1-x,1-y,1-z; #5 1+x,y,z; #6 1+x,1+y,z for **2**; #1 1-x,2-y,1-z; #2 -1+x,y,z; #3 x,y,-1+z; #4 3-x,1-y,1-z for **3**.

Table S5 K_{sv} values for fluorescent detecting TNP.

Sample	K_{sv}/M^{-1}	Ref.
1	3.94×10^4	This work
2	4.78×10^4	This work
3	5.01×10^4	This work
$[Zn_2(tipe)(tpe)] \cdot 3MeOH \cdot 13H_2O$	2.08×10^4	[13]
$[Zn_4(\mu_3-OH)_2(BTC)_2(BBI_4PY)_2] \cdot 10H_2O$	2.94×10^4	[14]
$Cd(NDC)(H_2O)$	2.385×10^4	[15]
$[Zn_2(L)(DMF)_3] \cdot 2DMF \cdot 2H_2O$ (H_4L =terphenyl-3,3'',5,5''-tetracarboxylic acid)	2.61×10^4	[16]

Table S6 Standard deviation and limit of detection (LOD) calculation for TNP in DMA suspension.

	1	2	3
1	753.432676	963.690498	944.961405
2	753.733048	963.882307	944.687457
3	753.873114	963.901308	944.858592
Standard deviation (σ)	0.22503	0.11661	0.13839
K_{sv} (m)	$3.94 \times 10^4 M^{-1}$	$4.78 \times 10^4 M^{-1}$	$5.01 \times 10^4 M^{-1}$
LOD ($3\sigma/m$)	$1.71 \times 10^{-5} M$	$7.32 \times 10^{-6} M$	$8.29 \times 10^{-6} M$

Table S7 Standard deviation and LOD calculation for TNP in H₂O suspension.

	1	2	3
1	864.656857	820.841933	617.724435
2	865.023295	821.048489	617.528418
3	865.078827	821.187064	617.988924
Standard deviation (σ)	0.22928	0.173678	0.23110
K_{sv} (m)	$5.88 \times 10^3 \text{ M}^{-1}$	$6.90 \times 10^3 \text{ M}^{-1}$	$2.13 \times 10^4 \text{ M}^{-1}$
LOD ($3\sigma/m$)	$1.17 \times 10^{-4} \text{ M}$	$7.55 \times 10^{-5} \text{ M}$	$3.25 \times 10^{-5} \text{ M}$

Table S8 Standard deviation and LOD calculation for 4-MB in DMA suspension of **2**.

	2
1	980.433837
2	980.887501
3	980.401471
Standard deviation (σ)	0.22188
K_{sv} (m)	$1.05 \times 10^5 \text{ M}^{-1}$
LOD ($3\sigma/m$)	$6.34 \times 10^{-6} \text{ M}$

Table S9 Standard deviation and LOD calculation for DBDPO in H₂O suspension.

	1	2	3
1	693.443260	869.070951	734.395858
2	693.975506	869.535634	734.982327
3	693.544505	869.519121	734.460143
Standard deviation (σ)	0.22928	0.21527	0.26263
K_{sv} (m)	$1.76 \times 10^2 \text{ M}^{-1}$	$1.33 \times 10^2 \text{ M}^{-1}$,	$2.62 \times 10^2 \text{ M}^{-1}$
LOD ($3\sigma/m$)	$3.91 \times 10^{-3} \text{ M}$	$4.86 \times 10^{-3} \text{ M}$	$3.01 \times 10^{-3} \text{ M}$

Table S10 Lifetimes of **1**, **2** and **3** dispersed in DMA or water before and after the addition of TNP solution.

Item	DMA			H ₂ O		
	1	2	3	1	2	3
Before quenching / ns	0.65	0.74	0.46	0.91	0.78	0.50
After quenching / ns	0.64	0.71	0.44	0.64	0.76	0.49

Table S11 Frontier molecular orbital energies for TNP and **1**, **2** and **3** at the generalized gradient approximation PerdewBurke-Ernzerhof (GGA-PBE) level of theory.

Samples	VB / eV	CB / eV	Energy Gap / eV
1	-5.474	-3.815	1.658
2	-6.290	-4.130	2.160
3	-6.399	-4.235	2.164
TNP	-7.430 (HOMO)	-5.240 (LUMO)	2.187

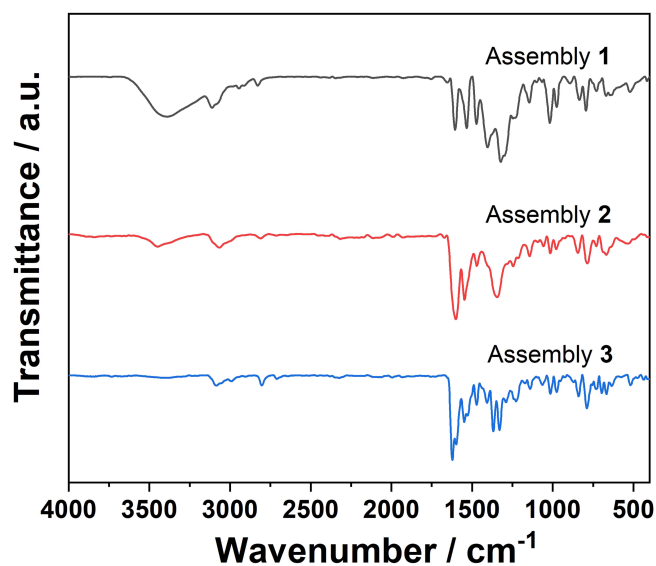


Fig. S1 FTIR-ATR spectra of **1**, **2** and **3**.

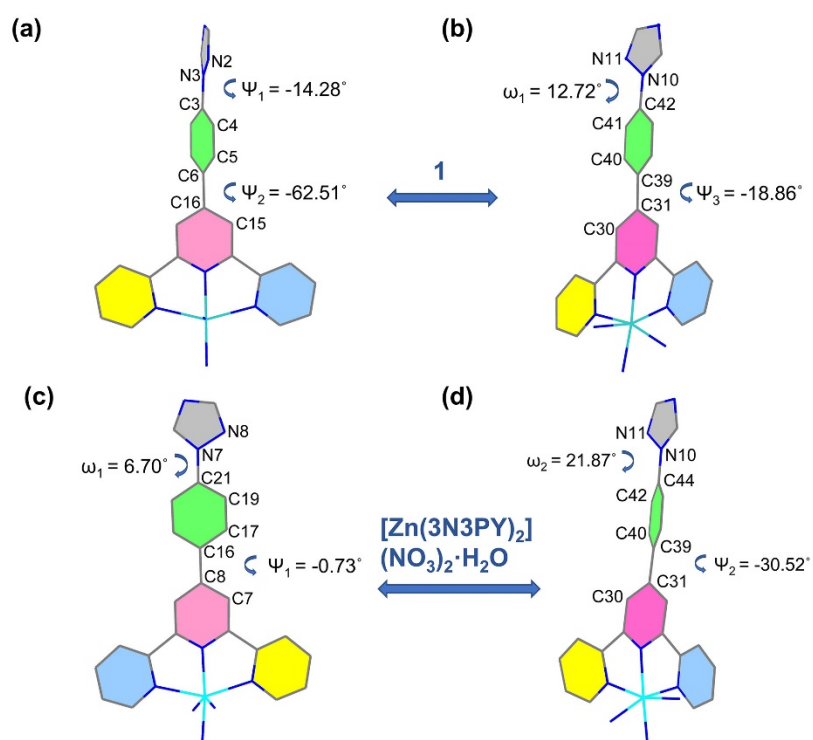


Fig. S2 Selected torsion angles ($^\circ$) for **1** viewing towards plane $(h, k, l) = (4, 4, -1)$ (a), $(4, -13, -1)$ (b) and reported $[\text{Zn}(\text{3N3PY})_2](\text{NO}_3)_2 \cdot \text{H}_2\text{O}$ to $(-1, -1, 3)$ (c) and $(-8, 5, -1)$ (d).

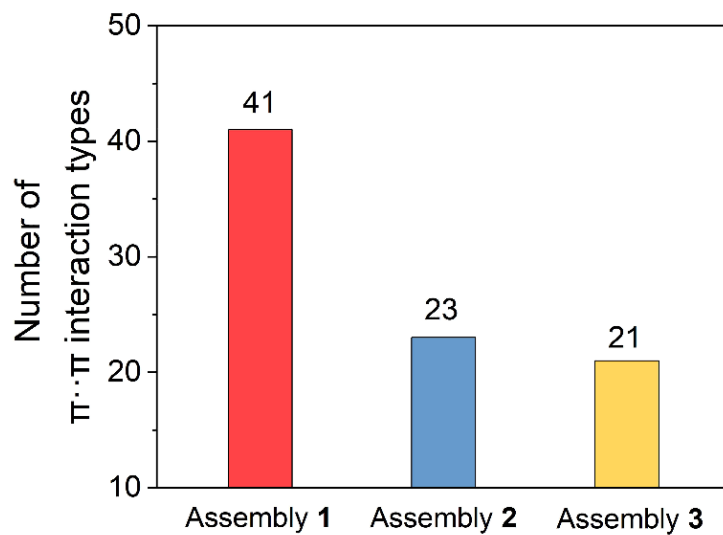


Fig. S3 The number of π - π interaction types for 1, 2 and 3.

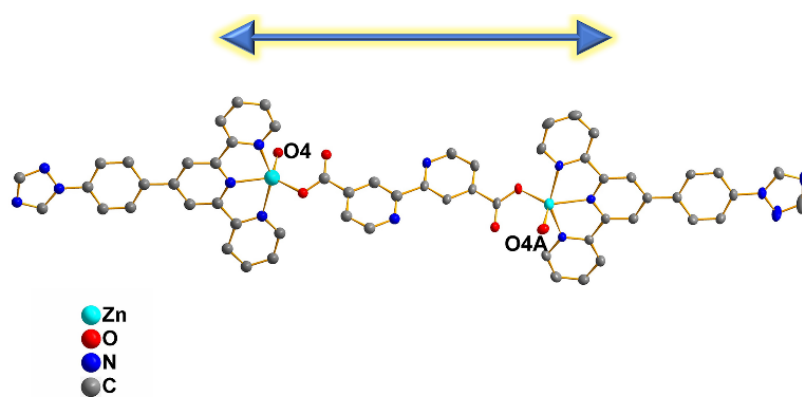


Fig. S4 Double-arrow unit in 2.

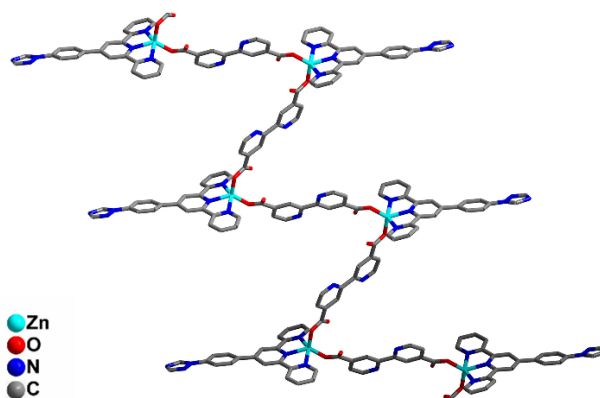


Fig. S5 1D chain structure of 2.

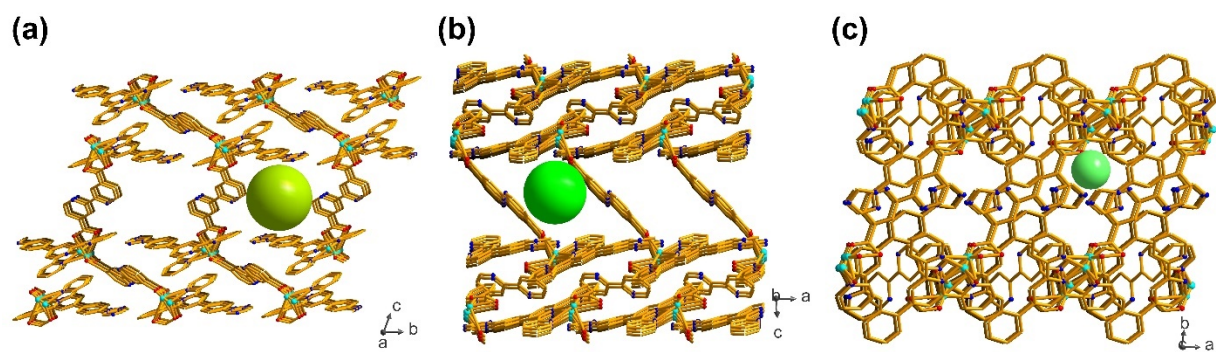


Fig. S6 The micropores in **2** by the stacking of 1D chains.

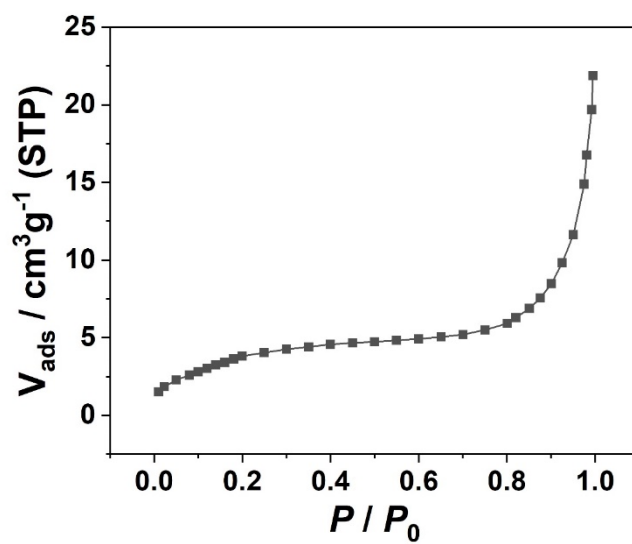


Fig. S7 N₂ adsorption isotherm at 77 K of assembly **2**.

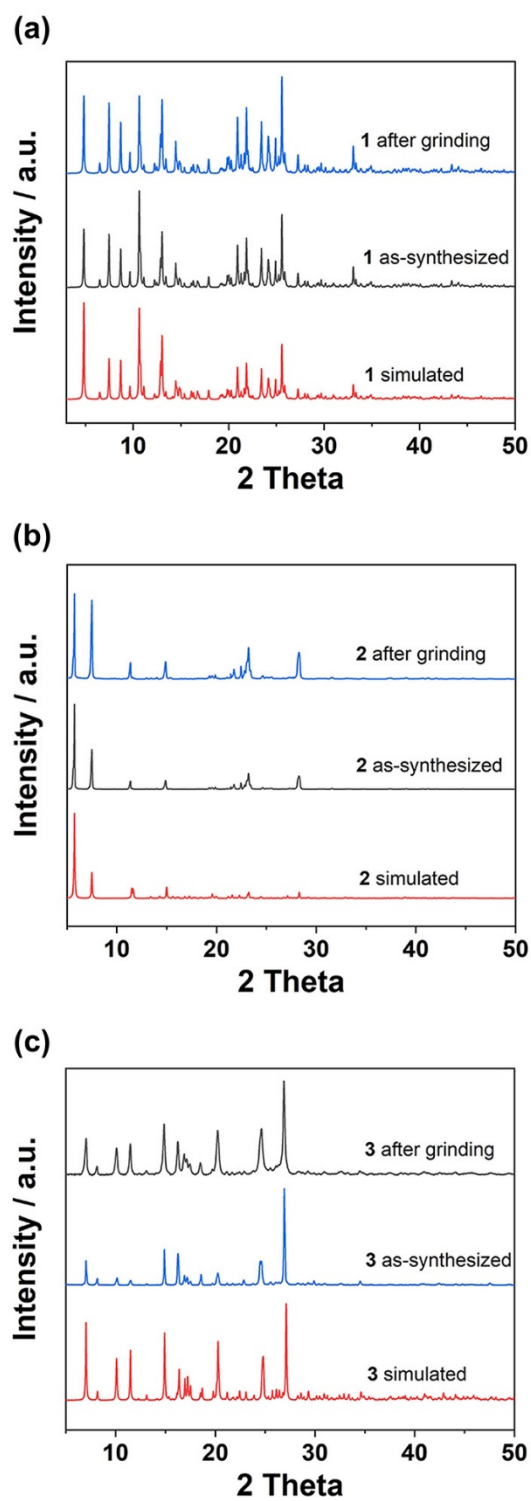


Fig. S8 PXRd patterns of **1** (a), **2** (b) and **3** (c).

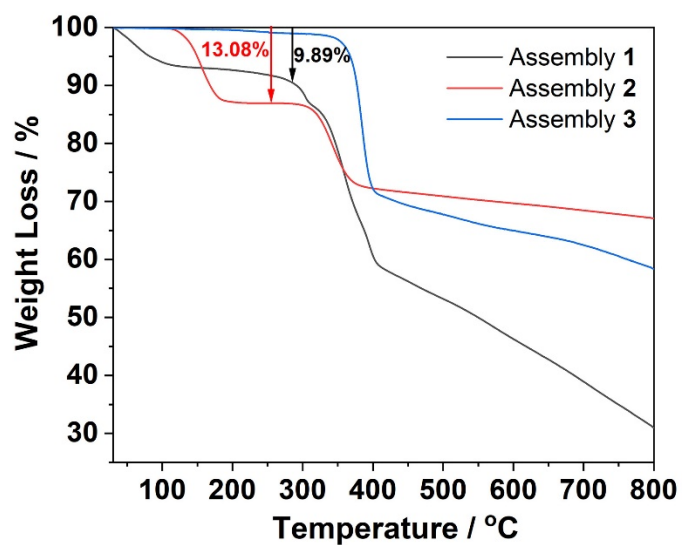


Fig. S9 TG curves of 1, 2 and 3.

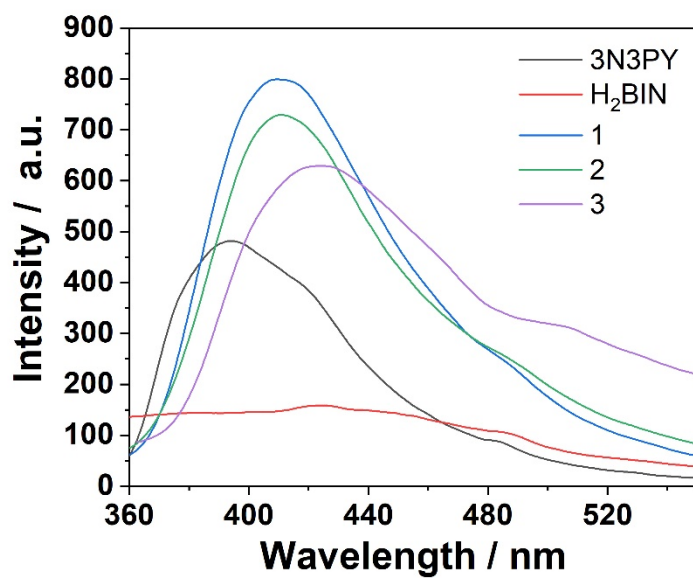


Fig. S10 Photoluminescence spectra of 3N3PY, H₂BIN, 1, 2 and 3 in solid state ($\lambda_{\text{ex}} = 330$ nm).

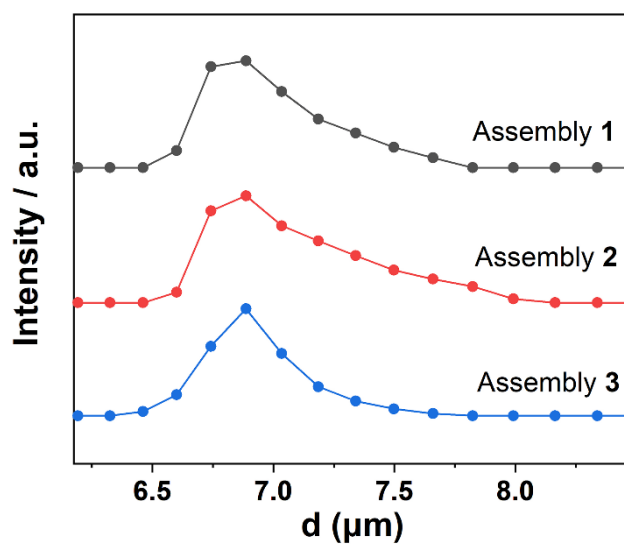


Fig. S11 DLS results of **1**, **2** and **3** in aqueous suspension.

The quenching efficiency (Φ) was determined by the following equation:

$$\Phi = 1 - I / I_0$$

where I_0 and I are the emission intensities without and with the presence of TNP.

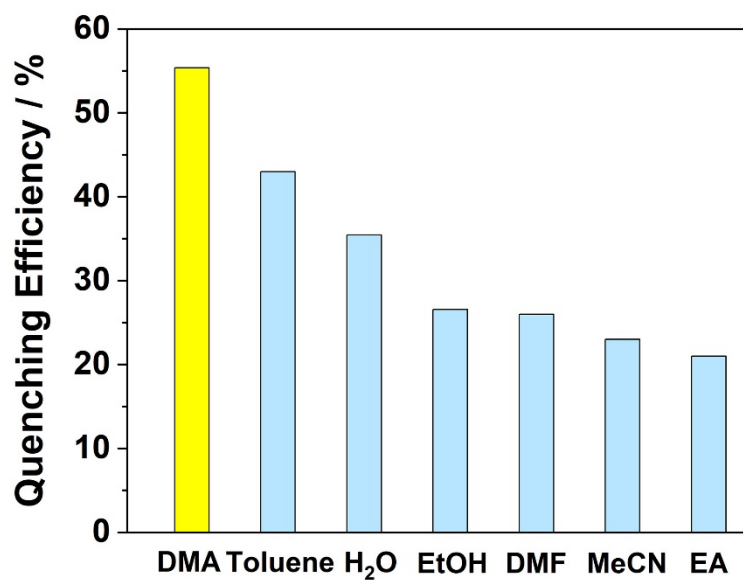


Fig. S12 Quenching efficiency ($1 - I / I_0$) of **1** by the corresponding TNP solution in different solvent.

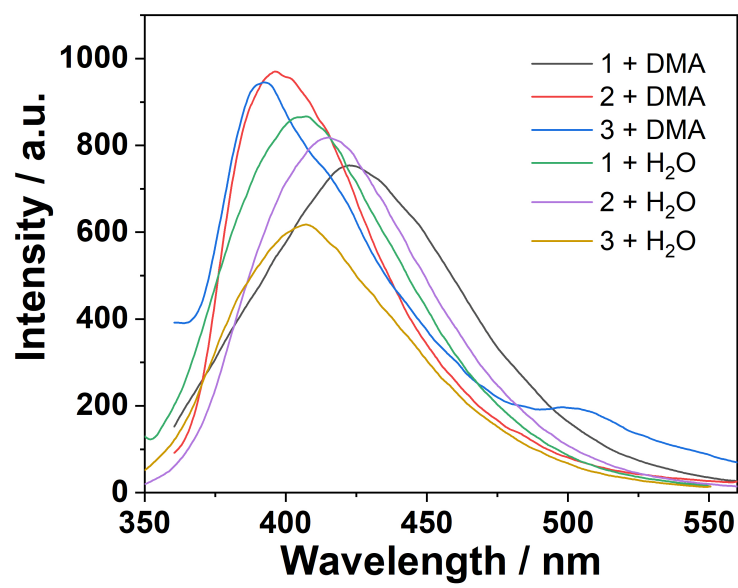


Fig. S13 Fluorescence spectra of 1, 2 and 3 suspended in DMA and H₂O.

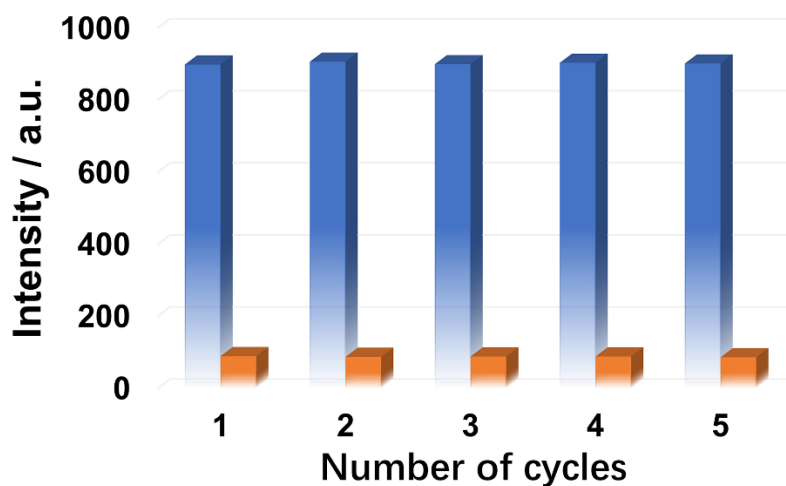


Fig. S14 Fluorescence quenching and repeatability test for **3** with initial fluorescence intensity (blue) and intensity after quenching (orange).

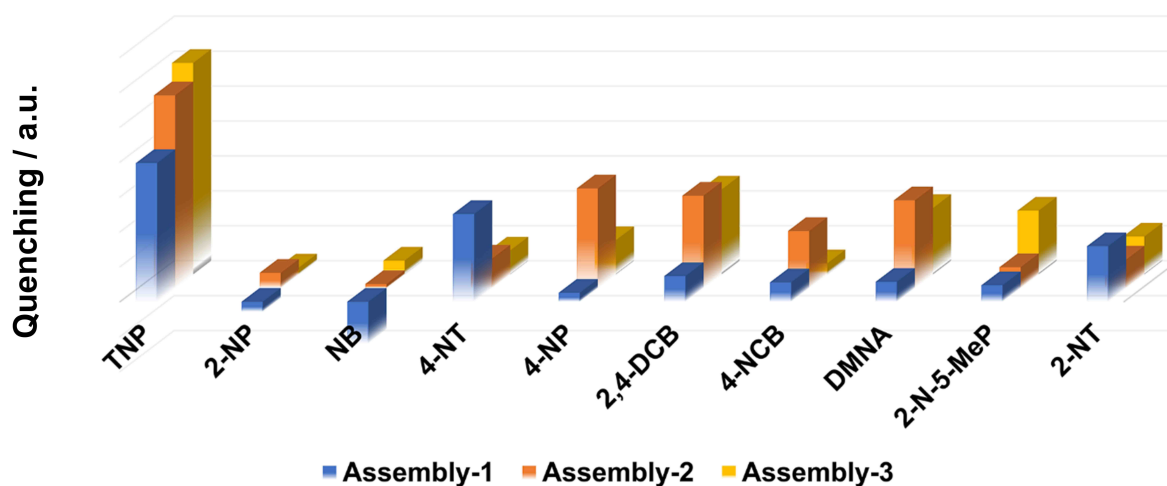


Fig. S15 Fluorescence quenching of **1**, **2** and **3** upon addition of the same amount of NACs including TNP, 2-nitrophenol (2-NP), nitrobenzene (NB), 4-nitrotoluene (4-NT), 4-nitrophenol (4-NP), 2,4-dinitrochloroben (2,4-DCB), 4-nitrochlorobenzene (4-NCB), 4,5-dimethyl-2-nitroaniline (DMNA), 5-methyl-2-nitrophenol (2-N-5-MeP) and 2-nitrotoluene (2-NT).

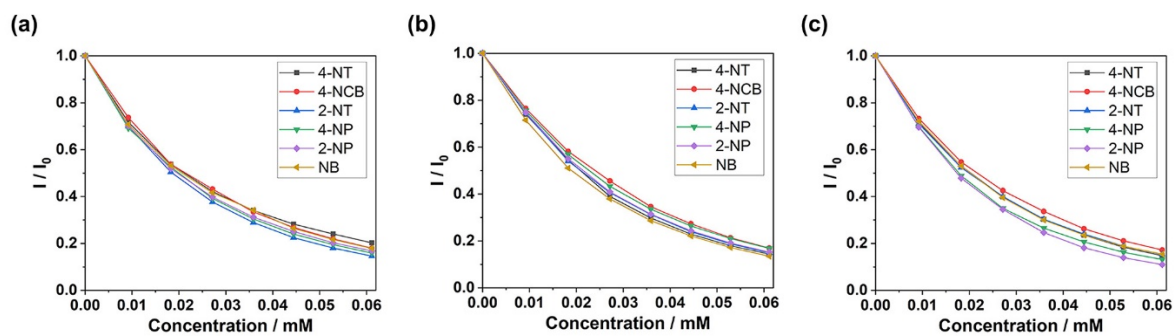


Fig. S16 Selective detection of TNP on **1** (a), **2** (b) and **3** (c) in the presence of other NACs in DMA suspensions.

The derivation process of the modified Stern-Volmer (S-V) equation is presented below.

Firstly, according to the previous report, the S-V equation was allowed to be written as a function of Φ as eqn. S1¹¹

$$\Phi = 1 - I / I_0 = 1 - 1 / (1 + K_{sv} Q_t) \quad (S1)$$

where Φ is quenching efficiency, K_{sv} is the S-V constant and Q_t is the uptake amount of the analyte vapour at time t by the sensor.

Accordingly, Q_t is reasonable to be replaced by eqn. S2 since the diffusion or adsorption-controlled process in a solid-state gas sensor can be described by a pseudo-second order kinetics.^{11,12}

$$Q_t = Q_\infty k_2 t / (1 + k_2 t) \quad (S2)$$

where Q_∞ is the uptake amount of analyte vapour at equilibrium and $k_2 = k Q_\infty$ with k to be the kinetic constant. The final modified S-V equation can be written as eqn. S3:

$$\Phi = K k_2 t / (1 + k_2 t + K k_2 t) \quad (S3)$$

where $K = Q_\infty \times K_{sv}$.

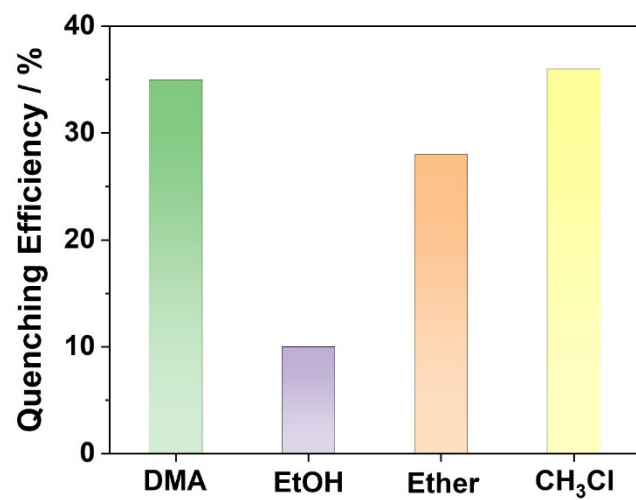


Fig. S17 Quenching efficiency ($1-I/I_0$) of **2** by adding 2 μ L 4-MB respectively in DMA, EtOH, ether, and chloroform (CH₃Cl) suspensions (0.5 mg/mL).

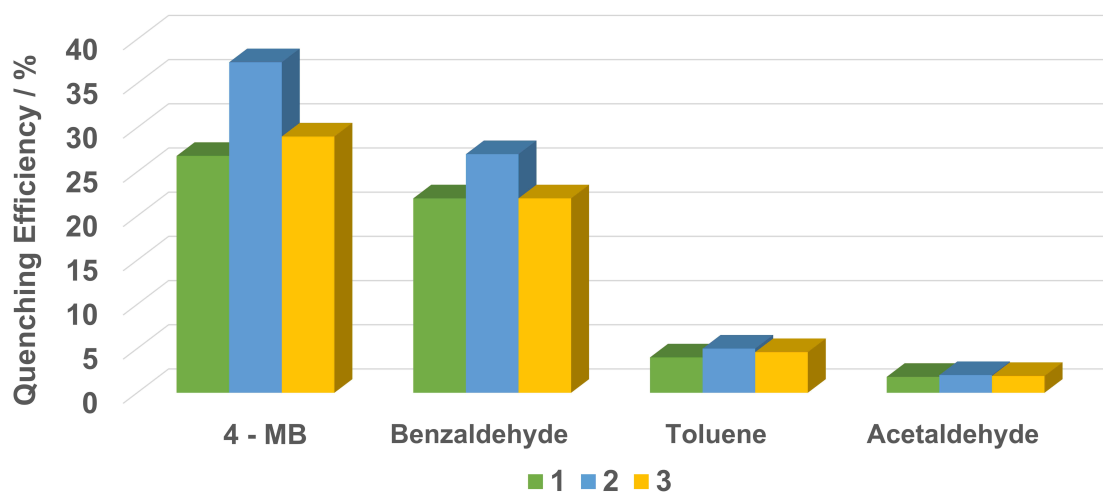


Fig. S18 Quenching efficiency ($1-I/I_0$) of **1, 2, 3** (0.5 mg/mL) for organic molecules.

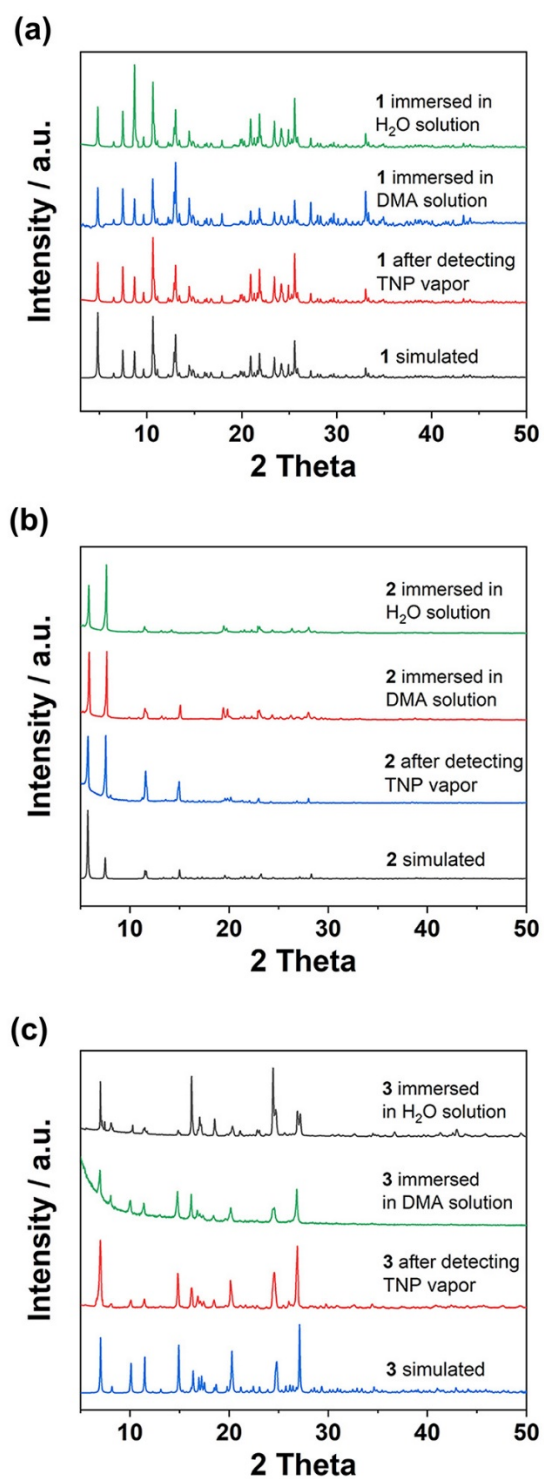


Fig. S19 PXR D patterns of **1** (a), **2** (b) and **3** (c) before and after immersing in H₂O or DMA solution of TNP and detecting TNP vapour.

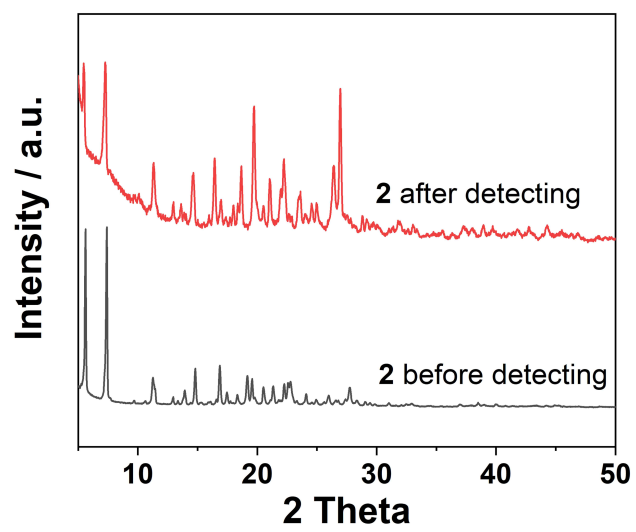


Fig. S20 PXR D patterns of **2** before and after detecting 4-MB.

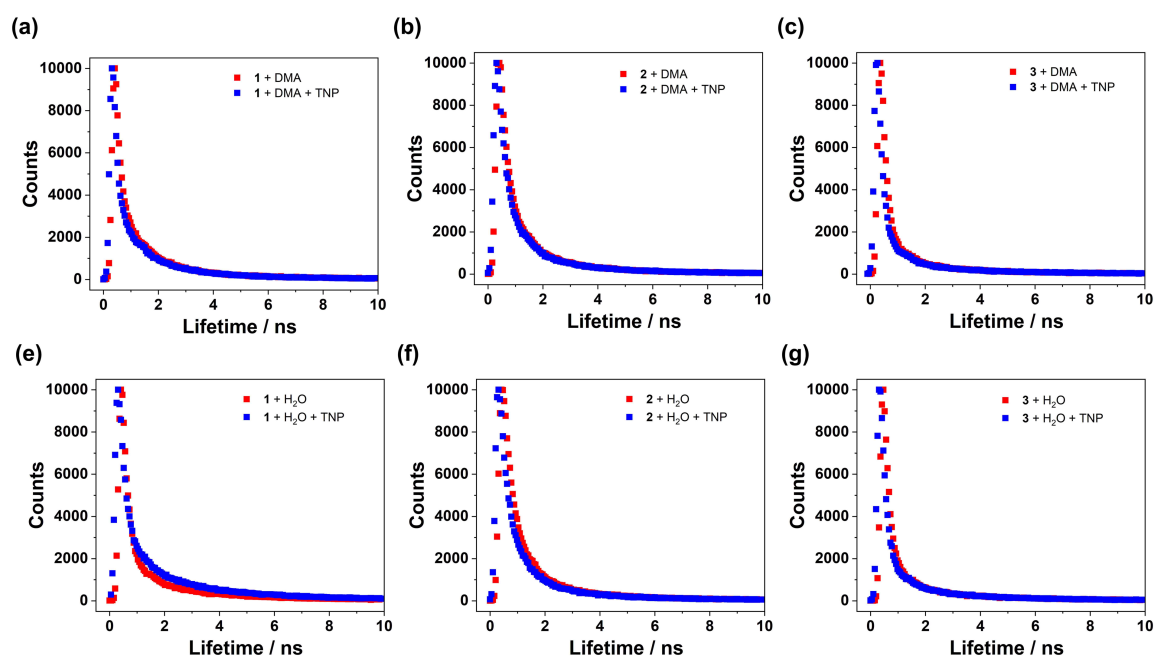


Fig. S21 Lifetimes of **1** (a), **2** (b) and **3** (c) dispersed in DMA before and after the addition of TNP solution. The solvent was changed to water for **1** (e), **2** (f) and **3** (g).

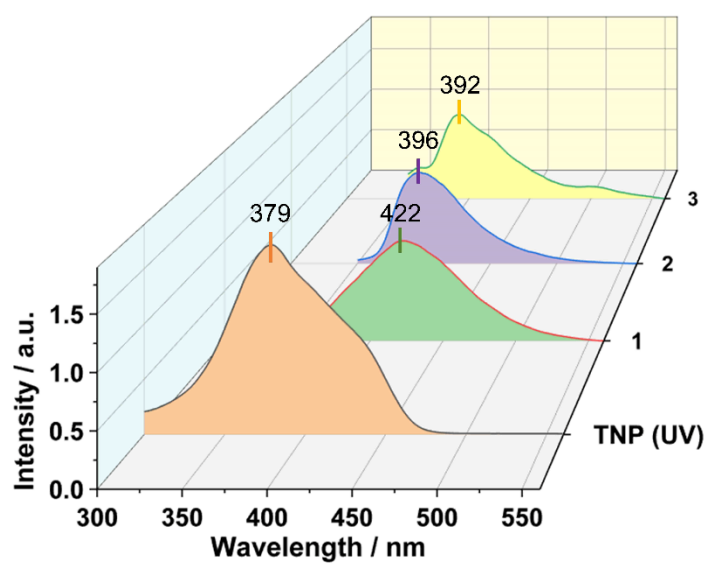


Fig. S22 Absorption spectra of TNP solution and normalized emission spectra of **1**, **2** and **3** stock suspension in DMA.

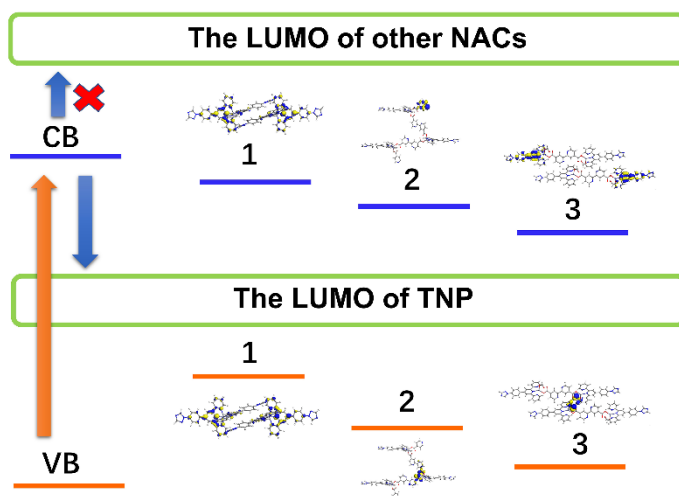


Fig. S23 Proposed PET process during the fluorescent quenching of **1**, **2** and **3** for TNP.

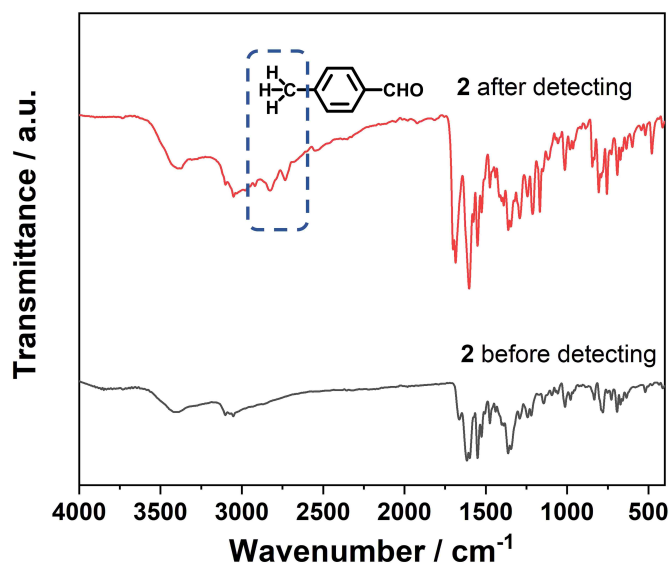


Fig. S24 FTIR-ATR spectra of **2** before and after detecting 4-MB.

References

- 1 SAINT, Program for Data Extraction and Reduction, Bruker AXS, Inc, Madison, WI, 2001.
- 2 G. M. Sheldrick, SADABS, Program for Empirical Adsorption Correction of Area Detector Data, University of Göttingen, Germany, 2003.
- 3 G. M. Sheldrick, SHELXT-2014, Program for the Crystal Structure Solution, University of Göttingen, Germany, 2014.
- 4 G. M. Sheldrick, SHELXL-2018, Program for the Crystal Structure Refinement, University of Göttingen, Germany, 2018.
- 5 D. S. P. Van and A. L. Spek, *Acta Cryst.* 1990, **46**, 194-201.
- 6 G. Ferey and C. Serre, *Chem. Soc. Rev.* 2009, **38**, 1380-1399.
- 7 J. M. Soler, E. Artacho, J. D. Gale, A. García, J. Junquera, P. Ordejón and D. Sánchez-Portal, *J. Phys.: Condens. Matter.* 2002, **14**, 2745-2779.
- 8 J. P. Perdew, K. Burke and M. Ernzerhof, *Phys. Rev. Lett.* 1996, **77**, 3865-3868.
- 9 G. Román-Pérez and J. M. Soler, *Phys. Rev. Lett.* 2009, **103**, 096102.

- 10 P. Wang, Z. Li, G. C. Lv, H. P. Zhou, C. Hou, W. Y. Sun and Y. P. Tian, *Inorg. Chem. Commun.* 2012, **18**, 87-91.
- 11 F. G. Moscoso, J. Almeida, A. Sousaraei, T. Lopes-Costa, A. M. G. Silva, J. Cabanillas-Gonzalez, L. Cunha-Silva and J. M. Pedrosa, *J. Mater. Chem. C* 2020, **8**, 3626-3630.
- 12 J. P. Simonin, *Chem. Eng. J.* 2016, **300**, 254-263.
- 13 Z. F. Qiu, S. M. Zhao, Z. H. Xu, Y. Zhao, Z. L. Wang and W. Y. Sun, *Cryst. Growth Des.* 2021, **21**, 5306–5316.
- 14 K. Sheeba, D. Prasenjit and K. M. Sanjay, *Inorg. Chem.* 2020, **59**, 4588–4600.
- 15 G. Pritam, K. S. Sourav, R. Additi and B. Priyabrata, *Eur. J. Inorg. Chem.* 2015, **17**, 2851-2857.
- 16 J. C. Jin, J. Wu, Y. X. He, B. H. Li, J. Q. Liu, R. Prasad, A. Kumar and S. R. Batten, *CrystEngComm*, 2017, **19**, 6464-6472.